

# Time-resolved Spectroscopy of Interparticle Coulombic Decay Processes

Elke Fasshauer\* and Lars Bojer Madsen  
*Department of Physics and Astronomy, Aarhus University*  
*Ny Munkegade 120, 8000 Aarhus, Denmark*  
 (Dated: 11.04.2019)

Interparticle Coulombic Decay (ICD) processes are electronic decay processes initiated by inner valence shell excitation or ionization of weakly interacting systems including solvents, biomolecules and quantum dots in semiconductors. We report theory for time-resolved spectator resonant ICD processes. Following excitation by a short XUV pulse, the spectrum of the resonant ICD electron is modelled. The decay process is quenched at different time delays by a strong infrared laser pulse. The quenching initiates a regular ICD process, whose ICD electron signal can be measured without interference effects. The typical lifetimes of ICD processes allow for the observation of oscillations of the time- and energy-differential ionization probability. We propose to utilize this oscillation to measure lifetimes of electronic decay processes.

Interparticle Coulombic Decay (ICD) [1, 2] is an electronic decay process of ionized systems consisting of at least two weakly bonded units, be it atoms, molecules or clusters. ICD has been observed in multiple systems like noble gas clusters [3–6] and clusters of different solvent molecules like water [4, 5, 7] or ammonia [8–11]. It allowed to explain the repair mechanism of the enzyme photolyase [12] and was used to establish a more efficient double ionization strategy [13]. ICD is furthermore discussed as a source of slow electrons, which are most efficient in damaging the DNA after exposure to high energy radiation or radioactive materials in the human body [14–19]. In this work, we shed light on this fundamental process by offering a time-resolved perspective directly of the electron dynamics. Thereby we provide the first step towards controlling the decay process, which might contribute to an optimization of cancer therapy.

Due to developments in creating short pulses in the extreme ultraviolet (XUV) and x-ray domain [21] a time-dependent investigation of ICD processes is feasible. Fano profiles of the much faster Auger process were recently measured [22, 23]. A few time-resolved investigations of ICD have already been performed theoretically and experimentally, where the ions produced in the process were measured [24–31]. However, electrons can be measured with higher energy resolution than ions and grant direct access to the electron dynamics and interference during the process. In this work, we will therefore focus on the time evolution of the time- and energy-differential ionization probability, propose how it can be measured in experiment, and discuss how the decay lifetimes can be determined from the time-resolved signal.

In brief, the ICD process starts from a unit  $A$ , which is ionized in the inner valence shell. This vacancy is filled by an electron from the same unit and the excess energy is simultaneously transferred to a neighbouring unit  $B$ . The latter is consequently ionized by emission of the ICD electron. The two positively charged units undergo

a Coulomb explosion (see Fig. 1). A related process is initiated by an excitation of unit  $A$ . This resonant ICD (RICD) can be characterized by the behaviour of the excited electron: it either participates in the decay process or not. The respective processes are called participator RICD (pRICD) [32] and spectator RICD (sRICD) [32–37]. In this work, we will only consider the sRICD: Unit  $A$  is excited from the inner valence. The vacancy is then filled by an electron from the valence and the excess energy is used to ionize the neighbouring unit  $B$  (see Fig. 1). This process is usually characterized by lifetimes of several tens to hundreds of femtoseconds. After the sRICD process, the excited unit  $A$  decays via fluorescence within a few nanoseconds.

We propose to initiate a RICD process by exciting with a short extreme ultraviolet (XUV) pulse. The system will then decay under emission of an RICD electron. This is illustrated in Fig. 1 for the case of the neon dimer after an excitation to the  $\text{Ne } 2s^{-1}5p$  state. At a later time  $t_s$ , a second short and intense infrared laser pulse quenches the RICD process by ionization. By varying the time delay  $t_s$  one should be able to observe the time-dependent formation of the RICD signal similar to the Auger process measured in Ref. [22]. The spectrum includes an oscillation in both the kinetic energy of the emitted electron as shown in Fig. 1a) and in time. At the same time, the proposed quenching would initiate an ICD process involving the excited ion  $A^{+*}$ . Due to the strong field ionization initiating the process, the signal would be interference free and therefore show a Lorentzian lineshape (see inset c) of Fig. 1). The position of this pure signal will allow to study the nuclear dynamics occurring before and during the RICD process.

The relevant property for the description of the time evolution of the ICD processes is the time- and energy-differential ionization probability obtained from the time-dependent wavefunction  $|\Psi(t)\rangle$  by  $P(E, t) = |\langle E|\Psi(t)\rangle|^2$ . Here  $|E\rangle$  denotes a continuum state with energy  $E$ , which entails both the kinetic energy of the emitted electron and the energy of the final cationic state. These continuum states are orthogonal to all bound states of the system. Atomic units are used throughout unless stated

---

\* elke.fasshauer@phys.au.dk

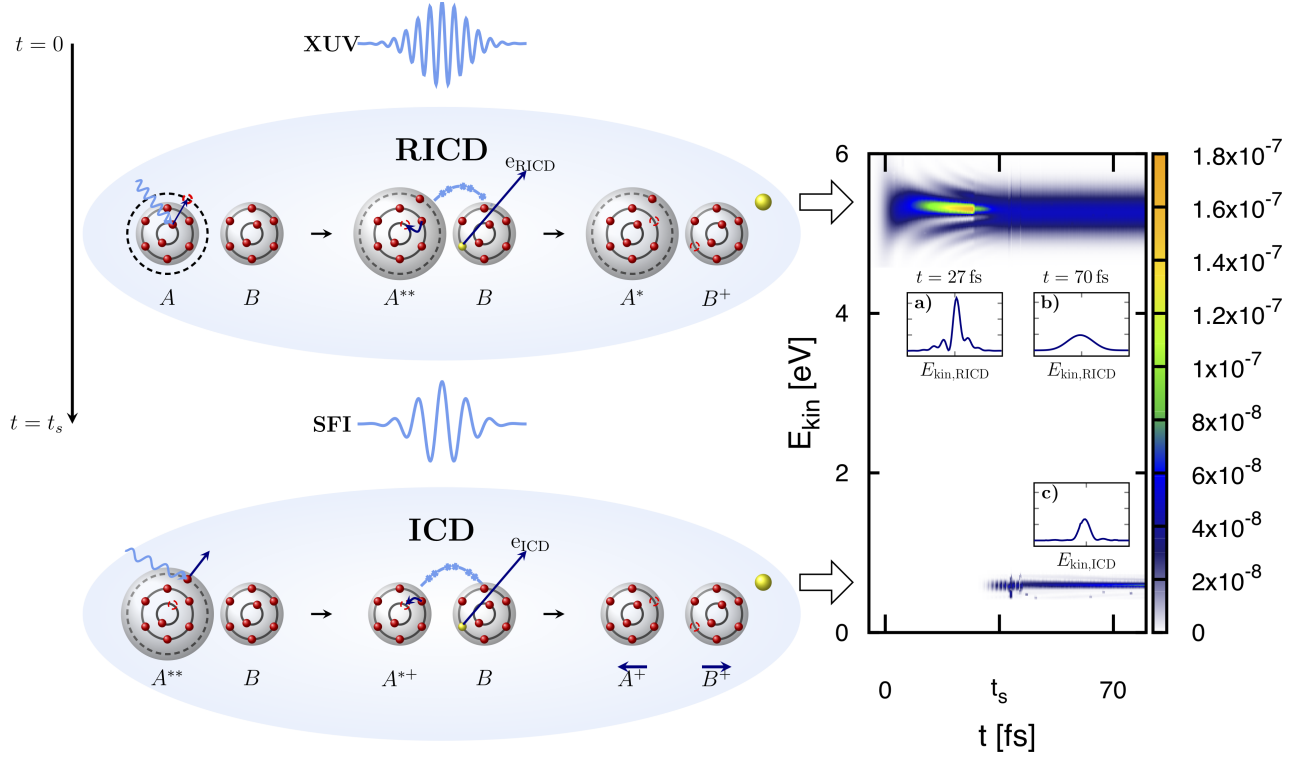


FIG. 1. Illustration [20] of the considered process. At  $t = 0$ , a spectator Resonant Interparticle Coulombic Decay (sRICD) is initiated by XUV excitation. At a later time  $t_s$  a second strong infrared laser pulse quenches the RICD process by ionization and thereby initiates ICD. The signals of the respective electrons with kinetic energies  $E_{\text{kin}}$  are well separated. While the RICD appears from the start of the XUV pulse centered at  $t = 0$ , the ICD signal appears after the second pulse. This approach allows for a time-resolved measurement of the RICD signal and an interference free measurement of the ICD signal. **RICD**: Unit A is excited from the inner valence shell. The created vacancy is filled with an electron from the outer valence and the excess energy is simultaneously transferred to B, which emits the RICD electron. **ICD**: The inner valence vacancy is created by removing the excited electron in A. It is then filled by an electron of the outer valence of A while the excess energy is transferred to B, which consequently emits the ICD electron. The two units are both positively charged and therefore undergo Coulomb explosion. **Spectrum**: The RICD signal centered around 5.3 eV before the second pulse shows the buildup of a Fano profile, with an additional oscillation in energy  $\cos[(E_{\text{kin}} + E_{\text{fin}} - E_r)t]$  (see inset a) and text). After depopulation of the RICD resonant state around  $t_s$ , only the direct term of Eq. (3) with a Gaussian shape remains (see inset b)). For the ICD signal centered around 0.6 eV shown in inset c), only the resonant term of Eq. (3) contributes, which has a Lorentzian shape.

otherwise.

We obtain the wavefunction of the system by solving the time-dependent Schrödinger equation  $i\partial_t |\Psi(t)\rangle = H(t) |\Psi(t)\rangle$  for a model system consisting of the ground state  $|G\rangle$ , the resonant state  $|R\rangle$  for the RICD and the resonant state  $|I\rangle$  for the ICD process, as well as two sets of continuum states characterized by the respective final state energy of the decay process. The Hamiltonian consists of the single configuration Hamiltonian  $H_0$ , the residual configuration interaction operators  $V_{\text{RICD}}$  and  $V_{\text{ICD}}$ , and the operator  $H_X(t)$  of the exciting XUV pulse:

$$H(t) = H_0 + V_{\text{RICD}} + V_{\text{ICD}} + H_X(t). \quad (1)$$

The effect of the ionizing infrared pulse is modelled by terminating the RICD and starting the ICD process at the time of the second pulse  $t_s$ . We will come back to this point below.

The continuum state of the RICD can couple to other continuum states under emission of a photon. This process is usually several orders of magnitudes slower than the electronic decay process and is therefore ignored in this work. We assume low field strengths of the XUV pulse and therefore use first order perturbation theory to describe its interaction with the system. Hence, the wavefunction evolves according to

$$|\Psi(t)\rangle = \tilde{U}(t, t_0) |G(t_0)\rangle - i \int_{-\infty}^t dt' \tilde{U}(t, t') H_X(t') |G(t')\rangle. \quad (2)$$

Here,  $\tilde{U}(t, t_0)$  is the time evolution operator from a time  $t_0$  until time  $t$  of the unperturbed system pertaining to the first three terms on the right hand side of Eq. (1).

We are free to choose an energy reference and therefore

set  $E_G = 0$ . Suppressing all dependences on angular

momentum leads to an amplitude of the RICD process for the resonance  $|R\rangle$  consisting of three terms

$$\begin{aligned} \langle E|\Psi(t)\rangle = & -i \int_{t_0}^t dt' \langle E|U_0(t, t')H_X(t')|G\rangle - \int_{t_0}^t dt' \int_{t'}^t dt'' \langle E|U_0(t, t'')|E\rangle V_{ER} \langle R|U_F^R(t'', t')|r\rangle \langle R|H_X(t')|G\rangle \\ & - \int_{t_0}^t dt' \int_{t'}^t dt'' \int dE' \langle E|U_0(t, t'')|E\rangle V_{ER} \langle R|U_F^R(t'', t')|E'\rangle \langle E'|H_X(t')|G\rangle. \end{aligned} \quad (3)$$

In these expressions,  $U_0(t, t')$  is the free particle time evolution operator.  $V_{ER} = \langle E|V|R\rangle = \sqrt{\Gamma_R/(2\pi)}$  is related to the decay rate of the resonant state  $\Gamma_R$  and  $U_F^R(t'', t')$  is the Fano time evolution operator, which is specific to the RICD process. For a derivation and explicit expressions of the three amplitudes in Eq. (3), see the Supplementary Material [38].

The first part of Eq. (3) describes the direct excitation and ionization to the continuum state, while the second part describes the excitation from the ground state to the resonant state followed by a decay to the continuum state. The last term describes the direct excitation and ionization to the continuum state, which couples to the resonant state, which then again decays into the continuum state. The interference of these different terms leads to the characteristic Fano profile [39].

We evaluated Eq. (3), see [38], and simulated the time-dependent build up of the Fano resonance for the RICD process of the neon dimer at the equilibrium distance of 3.08 Å [40] after an excitation to the  $\text{Ne}_2s^{-1}2p^65p_z$  state. All simulations were performed with ELDEST [41–45] using the parameters listed in Table I and choosing the Fano parameter  $q = 10$ . The exact  $q$  value is unknown to us, but we expect it to be larger than unity due to the low probability for direct single photon ionization

and excitation. We have performed calculations for a range of  $q$  parameters and the main conclusions remain unchanged [38].

We choose a Gaussian XUV pulse shape, and describe the interaction in the length gauge and dipole approximation such that  $H_X(t') = -E_X(t')\mu$  with  $\mu$  the dipole operator and  $E_X(t') = -\partial_{t'}\{A_{0X} \cos(\Omega t') \exp[-t'^2/(2\sigma_X^2)]\}$ , where  $\sigma_X = n_x\pi/\Omega\sqrt{\ln 2}$ . The exciting pulse for the results in Fig. 1 has  $A_{0X} = 5 \times 10^8 \text{ W/cm}^2$ ,  $\Omega = 47.6930 \text{ eV}$ , and a FWHM = 6.1 fs corresponding to 50 cycles.

We assumed a complete population transfer from the resonant state of the RICD process to the resonant state of the ICD process during the second ionizing pulse over a time of 15 fs as realized experimentally[22]. For this we assumed a Gaussian shaped change in the population of either of the two resonant states and that the ICD signal is unaffected by pulse shape effects [38]. Since we assume a direct population of the resonant state of the ICD process  $|I\rangle$  from the resonant state of the RICD process  $|R\rangle$  with a short and intense laser pulse, we assume, that the terms of Eq. (3), which are mediated by the continuum, can be neglected. After the end of the ionizing pulse the amplitude of the ICD process associated with resonance  $|I\rangle$  therefore reads

$$\langle E|\Psi(t)\rangle = - \int_{t_0}^t dt_s \int_{t_s+\delta t}^t dt'' \langle E|U_0(t, t'')|E\rangle V_{EI} \langle I|U_F^I(t'', t_s)|I\rangle \sqrt{N_0}, \quad (4)$$

where  $N_0$  is the population in  $|R\rangle$  at  $t_s - \delta t$ , with  $\delta t$  being half the duration of the infrared pulse [38]. Equation (4) shows that the ICD channel is populated without any interference, and we therefore obtain a pure Lorentzian profile in Fig. 1c). After the second pulse, the resonant state of the RICD process is totally depopulated. Therefore, only the direct term contributes to the signal yielding a Gaussian as shown in Fig. 1b).

In the investigation of decay processes with short laser

pulses, the shortness comes with the cost of an energy broadening. As a consequence, the kinetic energy spectrum of an RICD electron is given by a Fano profile centered around the kinetic energy, that corresponds to the energy of the resonant state, convoluted with a Gaussian centered around the kinetic energy, that would correspond to a direct excitation and ionization into the final state [38]. Here, we show the Lorentzian part inherent to

TABLE I. Energies and lifetimes for the three excited states  $\text{Ne}2s^{-1}2p^6np - \text{Ne}$  ( $n = 3, 4, 5$ ) undergoing RICD. The resonant energies are taken from Ref. [46], the final state energies of  $\text{Ne}2s^22p^5(P_{3/2,1/2})np - \text{Ne}2p^5(P_{3/2,1/2})$  and the ICD process were averaged to give approximations of non-relativistic energies. The lifetimes,  $\tau$ , of the RICD are from Ref. [35] and the ICD lifetime are from Ref. [47].

	$n = 3$	$n = 4$	$n = 5$	ICD
$E_r$ [eV]	45.5470	47.1230	47.6930	48.4750
$E_{\text{fin}}$ [eV]	40.2452	41.8391	42.4138	47.8688
$\tau(2s^{-1}(np_z)^1\Sigma_u^+)$ [fs]	286	112	106	98

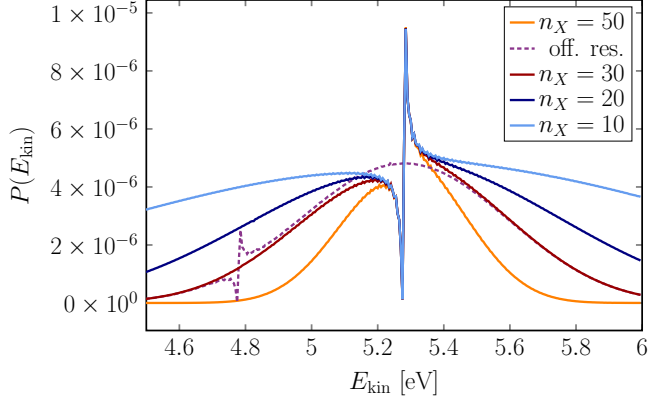


FIG. 2. Peak shape of the sRICD electron spectrum for late time  $t \rightarrow \infty$  after excitation of the  $5p$  state in the neon dimer depending on the number of cycles of the exciting pulse  $n_X$ . The shape can be explained by folding the Fourier transform of the exciting pulse in time with a Fano profile. In this example, the Fano  $q$  parameter is  $q = 1$ . Around the resonance energy, the peaks are identical. The width of the peak is determined by the duration of the exciting pulse. The dashed line illustrates an excitation 0.5 eV off resonance for  $n_X = 30$ .

all terms.

$$P(E_{\text{kin}}, \infty) \propto \frac{\exp[-\sigma_t^2(E_{\text{kin}} + E_{\text{fin}} - \Omega)^2]}{(E_{\text{kin}} + E_{\text{fin}} - E_r)^2 + \frac{\Gamma_r^2}{4}} \quad (5)$$

The shape of the spectra are illustrated for different numbers of cycles  $n_X$  for the exciting pulse in Fig. 2. There, the mean pulse energy was chosen to be on resonance and therefore, the Fano profile is centered on the maximum of the Gaussian. It is clearly seen, how the peak is narrowed with an increased number of laser cycles in the exciting pulse. In order to only excite into a single state we choose  $n_X = 50$ , such that other excited states are outside  $3\sigma_E$  of the energy distribution of the exciting pulse. In future investigations of the interaction between several decaying resonant states, a smaller number of cycles will be appropriate.

For the case of an off-resonant excitation, the Fano profile and the Gaussian will not be centered around the same kinetic energy of the RICD electron and the RICD electron peak will be damped accordingly as illustrated by the dashed line of Fig. 2 for  $n_X = 30$ .

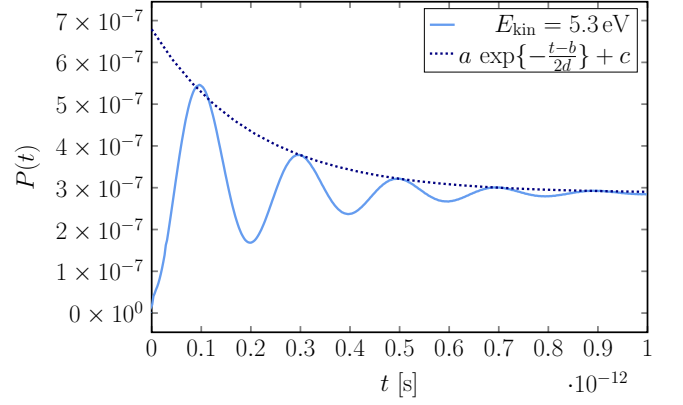


FIG. 3. Oscillation in time for observing the sRICD electron with a kinetic energy of 5.3 eV, for  $n_X = 50$  and  $q = 10$ . This oscillation can be described by  $\cos[(E_{\text{kin}} + E_{\text{fin}} - E_r)t]$ . Its period is therefore depending on the kinetic energy of the electron. It is damped in time by the decay of the resonant state  $\exp(-\Gamma_r t/2)$ . While the oscillations in energy are known and have been observed in energy, the oscillations in time require a process with a long enough lifetime to be observed around the resonance energy.

It can be shown analytically that, in addition to the overall structure at infinite times, the RICD and ICD spectra show an oscillation in both energy and time, which is proportional to [38]

$$\cos[(E_r - E_{\text{kin}} - E_{\text{fin}})t] \exp(-\frac{\Gamma_r}{2}t), \quad (6)$$

where  $r = R, I$ . The variation in energy, illustrated in Fig. 1a), is in agreement with Ref. [48].

As can be seen from Eq. (6), the oscillation is also visible in time as shown in Fig. 3 for a fixed kinetic energy of the RICD electron of  $E_{\text{kin}} = 5.3$  eV. Such an oscillation has not been observed close to resonance, where the signal is strongest, so far, because it requires long enough lifetimes of the resonant state. The electronic decay processes, that were studied in a time-resolved manner, are the much faster Auger processes [22, 23, 49–54]. The slower RICD process now offers the opportunity to observe and utilize it. The kinetic energy in Fig. 3 is slightly higher than the kinetic energy corresponding to the resonant state. The further away from the resonance this energy is chosen, the shorter the period of this oscillation. The oscillation is exponentially damped by the lifetime of the decaying state. However, the dynamics of the system are more complex than shown in Eq. (6), because some terms are damped by  $\exp(-\Gamma_r t)$  and some are damped by  $\exp(-\Gamma_r t/2)$ . Therefore, a fit of the maxima at longer times, where the parts damped by  $\exp(-\Gamma_r t)$  can be neglected, to the function  $a \exp[-(t-b)/2d] + c$  gives a good estimate of the lifetime  $d \approx \tau_r$ . The fit in Fig. 3, where the first maximum was omitted, yields a lifetime of 102 fs. This value is slightly lower, than 106 fs, but matches the input value used in the simulation very well. This kind of fit can therefore be used to determine the lifetime of

the electronic decay process.

We have presented a time-dependent theoretical description of the RICD and ICD processes investigated with short laser pulses. We suggest RICD as the primary process. The RICD is then quenched by a strong field pulse and ICD is initiated interference free. We have shown an oscillation of the ionization probability in time,

which is general for electronic decay processes. For processes with comparably long lifetimes, such as the ICD processes, this oscillation allows for a new way of measuring the lifetime of the underlying process.

The research of E.F. was supported by the Villum Foundation. The research of L.B.M. was supported by the Villum Kann Rasmussen Centre of Excellence QUSCOPE - Quantum Scale Optical Processes.

- 
- [1] L. S. Cederbaum, J. Zobeley, and F. Tarantelli, *Phys. Rev. Lett.* **79**, 4778 (1997).
  - [2] S. Marburger, O. Kugeler, U. Hergenhahn, and T. Möller, *Phys. Rev. Lett.* **90**, 4 (2003).
  - [3] R. Santra, J. Zobeley, L. S. Cederbaum, and N. Moiseyev, *Phys. Rev. Lett.* **85**, 4490 (2000).
  - [4] U. Hergenhahn, *J. Electron Spectrosc. Relat. Phenom.* **184**, 78 (2011).
  - [5] T. Jahnke, *J. Phys. B: Atomic, Molecular and Optical Physics* **48**, 082001 (2015).
  - [6] E. Fasshauer, *New J. Phys.* **18**, 043028 (2016).
  - [7] I. B. Müller and L. S. Cederbaum, *J. Chem. Phys.* **125**, 204305 (2006).
  - [8] N. V. Kryzhevoi and L. S. Cederbaum, *Angew. Chem. Int. Ed.* **50**, 1306 (2011).
  - [9] S. D. Stoychev, A. I. Kuleff, and L. S. Cederbaum, *J. Am. Chem. Soc.* **133**, 6817 (2011).
  - [10] N. V. Kryzhevoi and L. S. Cederbaum, *J. Phys. Chem. B* **115**, 5441 (2011).
  - [11] B. Oostenrijk, N. Walsh, J. Laksman, E. P. Mansson, C. Grunewald, S. L. Sorensen, and M. Gisselbrecht, *Phys. Chem. Chem. Phys.* **20**, 932 (2018).
  - [12] P. H. P. Harbach, M. Schneider, S. Faraji, and A. Dreuw, *J. Phys. Chem. Lett.* **4**, 943 (2013).
  - [13] V. Stumpf, K. Gokhberg, and L. S. Cederbaum, *Nature Chemistry* **8**, 237 (2016).
  - [14] B. Boudaïffa, P. Cloutier, D. Hunting, M. A. Huels, and L. Sanche, *Science* **287**, 1658 (2000).
  - [15] E. Brun, P. Cloutier, C. Sicard-Roselli, M. Fromm, and L. Sanche, *J. Phys. Chem. B* **113**, 10008 (2009).
  - [16] X. Pan, P. Cloutier, D. Hunting, and L. Sanche, *Phys. Rev. Lett.* **90**, 208102 (2003).
  - [17] F. Martin, P. D. Burrow, Z. Cai, P. Cloutier, D. Hunting, and L. Sanche, *Phys. Rev. Lett.* **93**, 068101 (2004).
  - [18] E. Surdutovich and A. V. Solov'yov, *Eur. Phys. J. D: Atomic, Molecular, Optical and Plasma Physics* **66**, 206 (2012).
  - [19] E. Alizadeh, T. M. Orlando, and L. Sanche, *Annu. Rev. Phys. Chem.* **66**, 379 (2015).
  - [20] E. Fasshauer, DOI:10.6084/m9.figshare.7808294.
  - [21] F. Krausz and M. Ivanov, *Rev. Mod. Phys.* **81**, 163 (2009).
  - [22] A. Kaldun, A. Blättermann, V. Stooß, S. Donsa, H. Wei, R. Pazourek, S. Nagele, C. D. Ott, C. Lin, J. Burgdörfer, and T. Pfeifer, *Science* **354**, 738 (2016).
  - [23] V. Gruson, L. Barreau, A. Jimenez-Galan, F. Risoud, J. Caillat, A. Maquet, B. Carre, F. Lepetit, J.-F. Hergott, T. Ruchon, L. Argenti, R. Taieb, F. Martin, and P. Salieres, *Science* **354**, 734 (2016).
  - [24] A. I. Kuleff and L. S. Cederbaum, *Phys. Rev. Lett.* **98**, 083201 (2007).
  - [25] K. Schnorr, A. Senftleben, M. Kurka, A. Rudenko, L. Foucar, G. Schmid, A. Broska, T. Pfeifer, K. Meyer, D. Anielski, R. Boll, D. Rolles, M. Kübel, M. F. Kling, Y. H. Jiang, S. Mondal, T. Tachibana, K. Ueda, T. Marchenko, M. Simon, G. Brenner, R. Treusch, S. Scheit, V. Averbukh, J. Ullrich, C. D. Schröter, and R. Moshhammer, *Phys. Rev. Lett.* **111**, 093402 (2013).
  - [26] F. Trinter, J. B. Williams, M. Weller, M. Waitz, M. Pitzer, J. Voigtsberger, C. Schober, G. Kastirke, C. Müller, C. Goihl, P. Burzynski, F. Wiegandt, T. Bauer, R. Wallauer, H. Sann, A. Kalinin, L. Schmidt, M. Schöffler, N. Sisourat, and T. Jahnke, *Phys. Rev. Lett.* **111**, 093401 (2013).
  - [27] K. Schnorr, A. Senftleben, G. Schmid, S. Augustin, M. Kurka, A. Rudenko, L. Foucar, A. Broska, K. Meyer, D. Anielski, D. Anielski, R. Boll, D. Rolles, M. Kübel, M. F. Kling, Y. H. Jiang, S. Mondal, T. Tachibana, K. Ueda, T. Marchenko, M. Simon, G. Brenner, R. Treusch, S. Scheit, V. Averbukh, J. Ullrich, T. Pfeifer, C. D. Schröter, and R. Moshhammer, *J. Electron Spectrosc. Relat. Phenom.* **204**, 245 (2015).
  - [28] U. Frühling, F. Trinter, F. Karimi, J. B. Williams, and T. Jahnke, *J. Electron. Spectrosc. Relat. Phenom.* **204**, 237 (2015).
  - [29] T. Mizuno, P. Cörlin, T. Miteva, K. Gokhberg, A. Kuleff, L. S. Cederbaum, T. Pfeifer, A. Fischer, and R. Moshhammer, *J. Chem. Phys.* **146**, 104305 (2017).
  - [30] T. Takanashi, N. V. Golubev, C. Callegari, H. Fukuzawa, K. Motomura, D. Iablonskyi, Y. Kumagai, S. Mondal, T. Tachibana, K. Nagaya, T. Nishiyama, K. Matsunami, P. Johnsson, P. Piseri, G. Sansone, A. Dubrouil, M. Reduzzi, P. Carpeggiani, C. Vozzi, M. Devetta, M. Negro, D. Faccialà, F. Calegari, A. Trabattoni, M. C. Castrovilli, Y. Ovcharenko, M. Mudrich, F. Stienkemeier, M. Coreno, M. Alagia, B. Schütte, N. Berrah, O. Plekan, P. Finetti, C. Spezzani, E. Ferrari, E. Allaria, G. Penco, C. Serpico, G. De Nino, B. Diviacco, S. Di Mitri, L. Giannessi, G. Jabbari, K. C. Prince, L. S. Cederbaum, P. V. Demekhin, A. I. Kuleff, and K. Ueda, *Phys. Rev. Lett.* **118**, 033202 (2017).
  - [31] Q. Jing and L. B. Madsen, *Phys. Rev. A* **99**, 013409 (2019).
  - [32] K. Gokhberg, V. Averbukh, and L. S. Cederbaum, *J. Chem. Phys.* **124**, 144315 (2006).
  - [33] S. Barth, S. Joshi, S. Marburger, V. Ulrich, A. Lindblad, G. Öhrwall, O. Björneholm, and U. Hergenhahn, *J. Chem. Phys.* **122**, 4 (2005).
  - [34] T. Aoto, K. Ito, Y. Hikosaka, E. Shigemasa, F. Penent, and P. Lablanquie, *Phys. Rev. Lett.* **97**, 243401 (2006).
  - [35] S. Kopelke, K. Gokhberg, L. S. Cederbaum, and V. Averbukh, *J. Chem. Phys.* **130**, 144103 (2009).

- [36] A. Knie, A. Hans, M. Förstel, U. Hergenhahn, P. Schmidt, R. Ph., C. Ozga, B. Kambs, F. Trinter, J. Voigtsberger, D. Metz, T. Jahnke, R. Dörner, A. I. Kuleff, L. S. Cederbaum, P. V. Demekhin, and A. Ehresmann, *New. J. Phys.* **16**, 102002 (2014).
- [37] A. Hans, L. B. Ltaief, M. Förstel, P. Schmidt, C. Ozga, P. Reiß, X. Holzapfel, C. Küstner-Wetekam, F. Wiegandt, F. Trinter, U. Hergenhahn, T. Jahnke, R. Dörner, A. Ehresmann, P. V. Demekhin, and A. Knie, *Chem. Phys.* **482**, 165 (2017).
- [38] See Supplemental Material, where the model is described in detail and where further illustrative results are given.
- [39] U. Fano, *Phys. Rev.* **124**, 1866 (1961).
- [40] A. Bondi, *J. Phys. Chem.* **68**, 441 (1964).
- [41] ELDEST version 2.0.2, Programme for the time-resolved investigation of electronic decay processes (2019), written by E. Fasshauer, DOI:10.5281/zenodo.2583910.
- [42] E. Jones, T. Oliphant, P. Peterson, *et al.*, “SciPy: Open source scientific tools for Python,” (2001–).
- [43] T. E. Oliphant, *Computing in Science & Engineering* **9**, 10 (2007).
- [44] K. J. Millman and M. Aivazis, *Computing in Science & Engineering* **13**, 9 (2011).
- [45] E. Fasshauer, (2019), input file, DOI:10.6084/m9.figshare.7808348.
- [46] A. Kramida, Y. Ralchenko, J. Reader, and N. A. T. (2018), “Nist atomic spectra database (version 5.6.1),” (2018), online.
- [47] A. Ghosh and N. Vaval, *J. Chem. Phys.* **141**, 234108 (2014).
- [48] M. Wickenhauser, *Ionization Dynamics of Atoms in Femto- and Attosecond Pulses*, Ph.D. thesis, Vienna University of Technology (2006).
- [49] M. Wickenhauser, J. Burgdörfer, F. Krausz, and M. Drescher, *Phys. Rev. Lett.* **94**, 023002 (2005).
- [50] T. Mercouris, Y. Komninos, and C. A. Nicolaides, *Phys. Rev. A* **75**, 013407 (2007).
- [51] C. A. Nicolaides, T. Mercouris, and Y. Komninos, *Phys. Rev. A* **80**, 055402 (2009).
- [52] W.-C. Chu and C. D. Lin, *Phys. Rev. A* **82**, 053415 (2010).
- [53] L. Argenti and E. Lindroth, *Phys. Rev. Lett.* **105**, 053002 (2010).
- [54] L. Argenti, R. Pazourek, J. Feist, S. Nagele, M. Liertzer, E. Persson, J. Burgdörfer, and E. Lindroth, *Phys. Rev. A* **87**, 053405 (2013).